iScience

CellPress
OPEN ACCESS

Article

# Alternatively activated lung alveolar and interstitial macrophages promote fungal growth

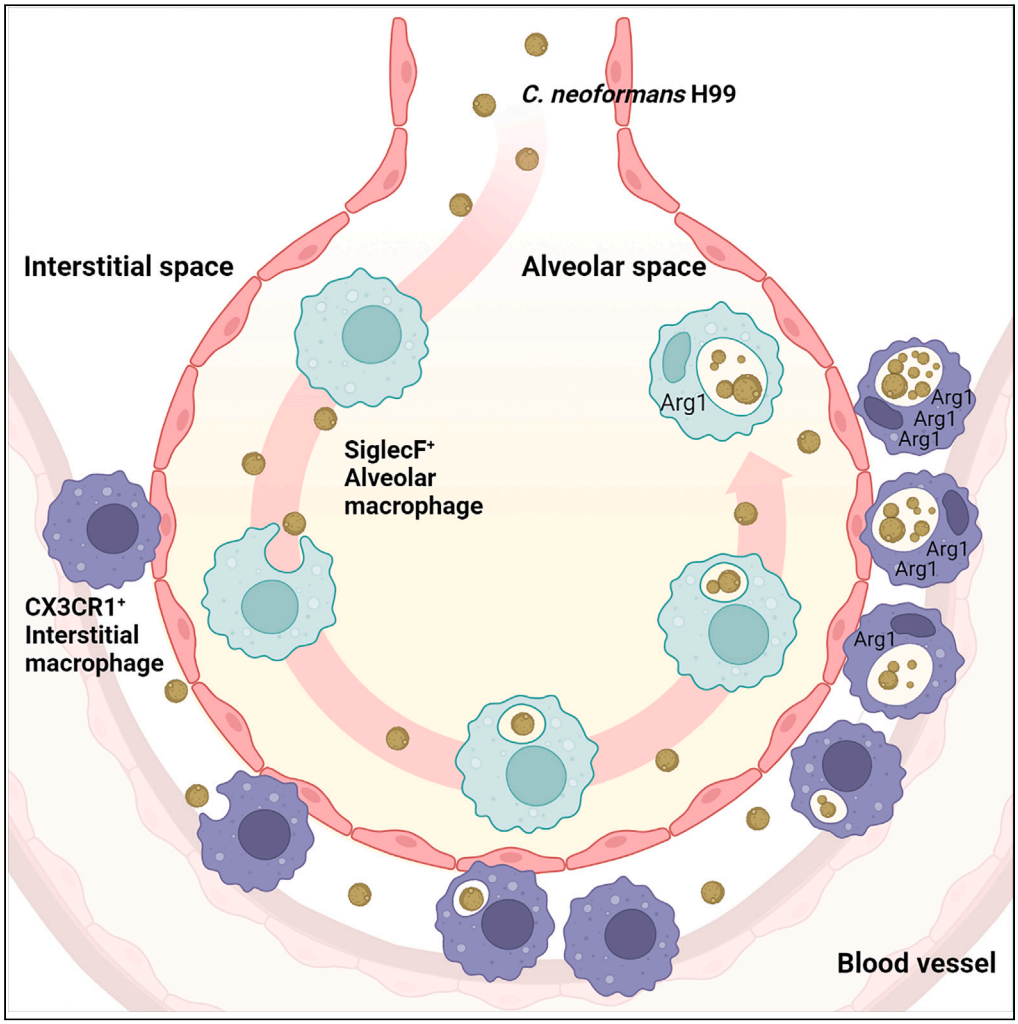


Ashley B. Strickland, Yanli Chen, Donglei Sun, Meiqing Shi

mshi@umd.edu

## Highlights

*C. neoformans* H99 is internalized by SiglecF$^+$ AMs and CX3CR1$^+$ IMs

*C. neoformans* H99 infection results in the expansion of IMs

*C. neoformans* H99 infection leads to alternative activation of AMs and IMs

Depletion of AMs or IMs reduces the pulmonary fungal loads

Strickland et al., iScience *26*, 106717
May 19, 2023 
https://doi.org/10.1016/j.isci.2023.106717

iScience

CellPress
OPEN ACCESS

Article

# Alternatively activated lung alveolar and interstitial macrophages promote fungal growth

Ashley B. Strickland,[1] Yanli Chen,[1] Donglei Sun,[1] and Meiqing Shi[1,2,*]

## SUMMARY

**How lung macrophages, especially interstitial macrophages (IMs), respond to invading pathogens remains elusive. Here, we show that mice exhibited a rapid and substantial expansion of macrophages, especially CX3CR1$^{+}$ IMs, in the lung following infection with *Cryptococcus neoformans*, a pathogenic fungus leading to high mortality among patients with HIV/AIDS. The IM expansion correlated with enhanced CSF1 and IL-4 production and was affected by the deficiency of CCR2 or Nr4a1. Both alveolar macrophages (AMs) and IMs were observed to harbor *C. neoformans* and became alternatively activated following infection, with IMs being more polarized. The absence of AMs by genetically disrupting CSF2 signaling reduced fungal loads in the lung and prolonged the survival of infected mice. Likewise, infected mice depleted of IMs by the CSF1 receptor inhibitor PLX5622 displayed significantly lower pulmonary fungal burdens. Thus, *C. neoformans* infection induces alternative activation of both AMs and IMs, which facilitates fungal growth in the lung.**

## INTRODUCTION

*Cryptococcus neoformans* is an encapsulated yeast found globally throughout the environment primarily in soil, avian excrement, and decaying material.[1] *C. neoformans* is acquired following the inhalation of spores or desiccated yeast.[2] Although the infection starts in the lung, the most devastating manifestation of *C. neoformans* infection occurs when this organism escapes the lungs and disseminates to the CNS.[3,4] If *C. neoformans* crosses the blood–brain barrier and enters the brain parenchyma, it can proliferate rapidly causing meningoencephalitis.[5,6] Left untreated, cryptococcal meningoencephalitis is fatal, and even with antifungal treatment, up to 20% of patients succumb within months of diagnosis.[7] The global incidence of cryptococcal meningoencephalitis is estimated to be more than 220,000 cases annually, with an associated 181,000 deaths each year.[8] Thus, containing the fungus in the lung and preventing extrapulmonary dissemination is essential for limiting *C. neoformans* pathogenesis. However, the mechanisms involved in fungal clearance and growth in the lung remain incompletely understood.

Macrophages are among the first immune cells to encounter invading pathogens in the lungs. Two distinct types of macrophages exist in the lungs of humans and mice: alveolar macrophages (AMs) and interstitial macrophages (IMs).[9,10] The most well characterized of these is AMs. AMs reside within alveolar spaces and are known as the first line of defense against inhaled pathogens.[11] In contrast, IMs are present in nonalveolar spaces including the lung parenchyma and bronchial interstitium.[12–14] Due to the fact that IMs are difficult to isolate,[12] these cells remain understudied and only until recently have studies begun to identify different subsets of IMs and their functions.[14–17] IMs produce high levels of IL-10 and are believed to primarily function as immunoregulatory cells.[18,19] Due to their phagocytic capacity and their expression of MHC class II, IMs may also possess antigen-presenting capabilities, and thus play a role in host defense.[12,19,20] Furthermore, studies are beginning to demonstrate that IMs differ to AMs in their response to pathogens;[9,21,22] however, how IMs respond to microbial infections still remains largely unknown.

During *C. neoformans* infection, AMs have been reported to phagocytose *C. neoformans*, but their ability to kill cryptococci was host species- and fungal strain-dependent.[23–26] In addition, AMs have also been implicated in facilitating the extrapulmonary dissemination of *C. neoformans*.[27,28] Following the initial interaction between AMs with *C. neoformans*, a substantial amount of myeloid cells, especially Ly6C$^{hi}$ inflammatory monocytes, are recruited to the infected lung and differentiate into exudate macrophages and inflammatory dendritic cells (DCs).[29,30] The functions of inflammatory monocytes have been well

[1]Division of Immunology, Virginia-Maryland College of Veterinary Medicine, Maryland Pathogen Research Institute, University of Maryland, College Park, MD 20742, USA

[2]Lead contact

*Correspondence: mshi@umd.edu

https://doi.org/10.1016/j.isci.2023.106717

characterized during *C. neoformans* infection.[31] Early studies have shown that inflammatory monocytes are required for protection;[32,33] however, later studies suggested that these monocytes are detrimental during acute infection with a highly virulent *C. neoformans* strain.[34,35] Regarding IMs, it has been reported that these cells harbored intracellular cryptococci following intratracheal instillation, suggesting these cells may contribute to host responses to *C. neoformans*.[9] A more recent study demonstrated that CPL1, a secreted cryptococcal protein, induces alternative activation of IMs, facilitating growth of *C. neoformans* within the phagocytes.[36] Nevertheless, it still remains incompletely understood as to how lung macrophages, particularly IMs, respond to *C. neoformans* infection and how they contribute to fungal clearance and growth in the infected lung.

In the current study, we developed a gating strategy to characterize lung-resident macrophages based on the cell surface markers recently identified by RNA-sequencing analyses.[14–17] Using this gating strategy, we found that cryptococcal infection induces the accumulation of $CD68^{hi}$ macrophages in the lungs of mice, which consist mainly of $CX3CR1^{+}$ IMs. $CD68^{hi}$ macrophages were seen to harbor fungal cells and became alternatively activated during infection. We found that inhibition of the CSF1 receptor (CSF1R) by PLX5622 can deplete IMs. Mice depleted of AMs or IMs displayed significantly lower fungal burdens in the lung during infection. Our data demonstrate that alternatively activated AMs and IMs promote fungal growth in the lung during *C. neoformans* infection.

## RESULTS

### *C. neoformans* infection induces the accumulation of $CD68^{hi}$ macrophages in the lungs of mice

To begin investigating the role of pulmonary macrophages during infection with *C. neoformans*, we first examined the distribution of these cells in the lungs of infected mice using immunohistochemistry. We found that detection of the macrophage marker F4/80 was difficult, and instead macrophages were most easily identified by CD68 (Figure 1A). With this in mind, we examined the distribution of $CD68^{+}$ cells in the lungs before and after infection with *C. neoformans* (Figure 1A). To confirm that these cells were bona fide macrophages, we assessed the expression of other known macrophage markers on $CD68^{+}$ cells using flow cytometry (Figure 1B). We observed two $CD68^{+}$ populations in the lungs of infected mice: a $CD68^{hi}$ and a $CD68^{lo}$ population. Based on their expression of MerTK, CD64, and F4/80, we determined that the $CD68^{lo}$ population consisted of monocytes ($CD68^{lo}MerTK^{lo}CD64^{lo}F4/80^{lo}$) and that the $CD68^{hi}$ population was composed of macrophages ($CD68^{hi}MerTK^{hi}$ $CD64^{hi}F4/80^{hi}$) (Figure 1B). This was further confirmed by the size and granularity of these cells, determined by forward and side scatter, respectively, where $CD68^{lo}$ monocytes were smaller and less granular ($FSC^{lo}SSC^{lo}$) and $CD68^{hi}$ macrophages larger and more complex ($FSC^{hi}SSC^{hi}$) (Figure 1B).

Having established a strategy to identify macrophages, we next quantified the number of these cells in the lungs of mice before and after cryptococcal infection and determined that $CD68^{hi}$ cells were present in the naive lung, and rapidly expanded in response to *C. neoformans* infection (Figures 1C and 1D). The number of $CD68^{hi}$ macrophages increased nearly 10-fold within the span of a week following infection, and reached their peak at 3 weeks post infection (PI) (Figure 1D); a time that coincides with the highest fungal burdens in the lung prior to mortality (data not shown). This suggests that macrophages may play an important role in the lungs during cryptococcal infection.

### Characterization of lung macrophages reveals that $CD68^{hi}$ macrophages in *Cryptococcus*-infected mice consist of AMs and IMs

To identify which macrophage subset(s) contributed to the $CD68^{hi}$ population, we immunophenotyped these cells 1-week PI using flow cytometry (Figures 2A and 2B). Upon closer inspection, we determined that a portion of these cells expressed high levels of SiglecF. This, along with their high expression of CD11c and lack of CD11b expression, indicated that these cells were AMs (Figures 2A and 2B). The remainder of the $CD68^{hi}$ cells was $SiglecF^{-}CD11b^{+}Ly6C^{int}CX3CR1^{+}$ (Figure 2A). These cells also expressed a number of canonical macrophage markers including MerTK, CD64, and F4/80 (Figure 2B), suggesting that these cells were IMs.[19]

Recent literature has identified several subsets of IMs, including IM1/IM2s ($CD11c^{lo}MHCII^{+}$) and IM3s ($CD11c^{hi}MHCII^{hi}$), $Lyve1^{hi}MHCII^{lo}$ and $Lyve1^{lo}MHCII^{hi}$ IMs, $CD206^{+}$ and $CD206^{-}$ IMs, and $CD169^{+}$ and $CD169^{-}$ IMs.[14–17] Growing evidence suggests that these subsets differ in their response to pathogenic stimuli.[37] For this reason, we sought to determine which IM subsets were present in the lungs of mice during

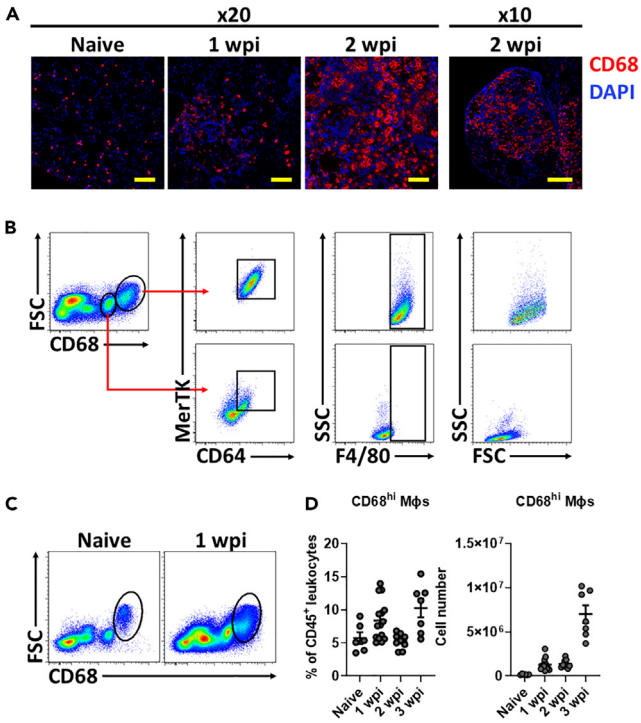


**Figure 1. *C. neoformans* infection induces the accumulation of CD68$^{hi}$ macrophages in the lungs of mice**

(A) Representative immunohistochemistry images of CD68$^{+}$ cell (red) distribution in the lungs of naive C57BL/6 mice, and mice infected intranasally with *C. neoformans* H99 at weeks 1 and 2 PI. Nuclei were stained with DAPI (blue). Scale bars: 100 μm for x20; 500 μm for x10.

(B) Representative flow cytometry plots characterizing CD68$^{+}$ cell expression of macrophage markers MerTK, CD64, F4/80, and forward scatter and side scatter at 1-week PI.

(C) Representative flow cytometry plots of CD68$^{hi}$ cells in the lungs of naive mice and infected mice at 1-week PI.

(D) The quantification of percentages and numbers of CD45$^{+}$CD68$^{hi}$ cells in the lungs of naive mice (n = 6) and mice infected with *C. neoformans* at weeks 1, 2, and 3 PI (n = 7–15). Data are expressed as mean ± SEM and are pooled from two independent experiments.

cryptococcal infection. Flow cytometric analyses revealed a single predominant IM population in the lung 1 week following infection. These cells were CD11c$^{+}$ and MHCII$^{+}$, but expressed both markers at lower levels than AMs. In addition, when compared to CD169$^{+}$ AMs,[15] IMs appeared to be CD169$^{lo/-}$ (Figure 2B). IMs also expressed similar levels of Lyve1 as AMs which have been reported to be Lyve1$^{lo}$,[14] indicating these IMs were also Lyve1$^{lo}$ (Figure 2B). It is noteworthy that IMs expressed CX3CR1, in agreement with previous findings that all IM subtypes are CX3CR1$^{+}$.[14,15,17] Taking these into account, we determined that IMs in the lung during infection with *C. neoformans* most closely resembled IM3s. The fact that these cells are also CD206$^{+}$ though, is in conflict with previously published literature that identifies IM3s as CD206$^{-}$ (Figures 2B and 2C). It is possible that during cryptococcal infection, CD206 expression instead reflects the activation status of these IMs.[38]

Using the aforementioned IM subset markers, we attempted to immunostain IM subsets in lung sections of infected mice. We determined that CD206 and CD11c were most readily detected, and that CD68$^{+}$ cells co-expressed both markers, thus confirming the results from our flow cytometry analyses and demonstrating that *C. neoformans* infection induces the accumulation of CD68$^{hi}$ AMs and IMs in the lungs (Figure 2C).

## The expansion of lung IMs correlates with increased CSF1 and IL-4 production and is affected by the deficiency of CCR2 or Nr4a1 during *C. neoformans* infection

Prior to infection with *C. neoformans*, approximately 88% of the CD68$^{hi}$ cells were AMs and less than 6% were IMs (Figure 3A). This is in agreement with reports that AMs are more abundant in the naive lung

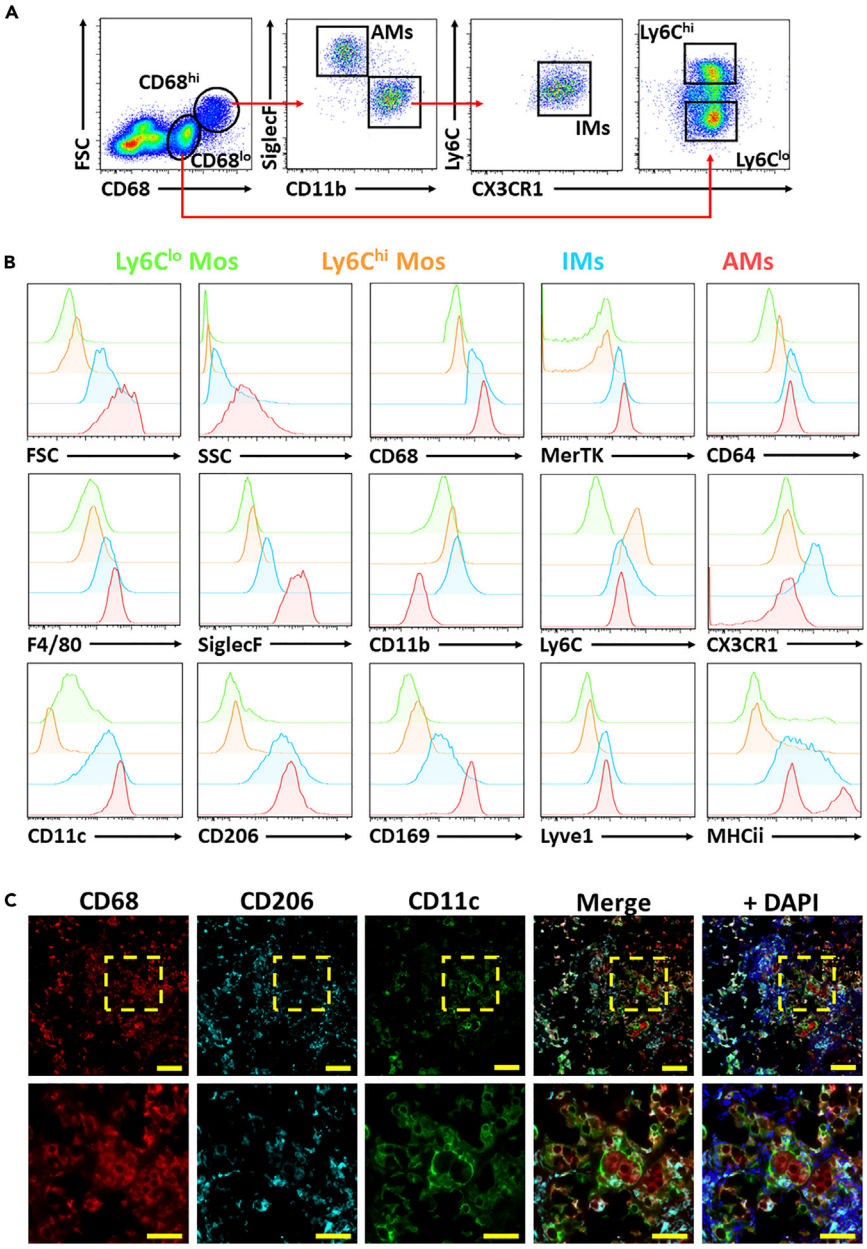


**Figure 2. Characterization of lung macrophages reveals that CD68$^{hi}$ macrophages consist of AMs and IMs during *C. neoformans* infection**

(A) Flow cytometry gating strategy to identify CD45$^{+}$CD68$^{hi}$SiglecF$^{+}$CD11b$^{-}$ alveolar macrophages (AMs), CD45$^{+}$CD68$^{hi}$SiglecF$^{-}$CD11b$^{+}$Ly6C$^{int}$CX3CR1$^{+}$ interstitial macrophages (IMs), CD45$^{+}$CD68$^{lo}$SiglecF$^{-}$CD11b$^{+}$Ly6C$^{hi}$ monocytes (Ly6C$^{hi}$), and CD45$^{+}$CD68$^{lo}$SiglecF$^{-}$CD11b$^{+}$Ly6C$^{lo}$ monocytes (Ly6C$^{lo}$) at 1-week PI.

(B) Representative histogram overlays of the expressions of various macrophages markers in AMs (red line), IMs (blue line), Ly6C$^{hi}$ monocytes (orange line), and Ly6C$^{lo}$ monocytes (green line) at 1-week PI.

(C) Representative immunohistochemistry images of CD68$^{+}$ (red), CD206$^{+}$ (blue), and CD11c$^{+}$ (green) cells in the lungs of infected mice at 2 weeks PI. Nuclei were stained with DAPI (blue). In the top row, sections were imaged at x20 and images in the bottom row are zoomed in on the areas within the yellow boxes. Scale bars: 100 μm (top); 50 μm (bottom).

than their IM counterparts.[14,37] However, following infection, IMs constituted more than 78% of this population, while AMs made up less than 17% (Figure 3A). These alterations in the composition of the CD68$^{hi}$ population were due to the dramatic changes in IM numbers following infection. At 1-week PI, there was a striking increase in the number of IMs in the lungs of infected mice (Figure 3B). IMs continued to expand

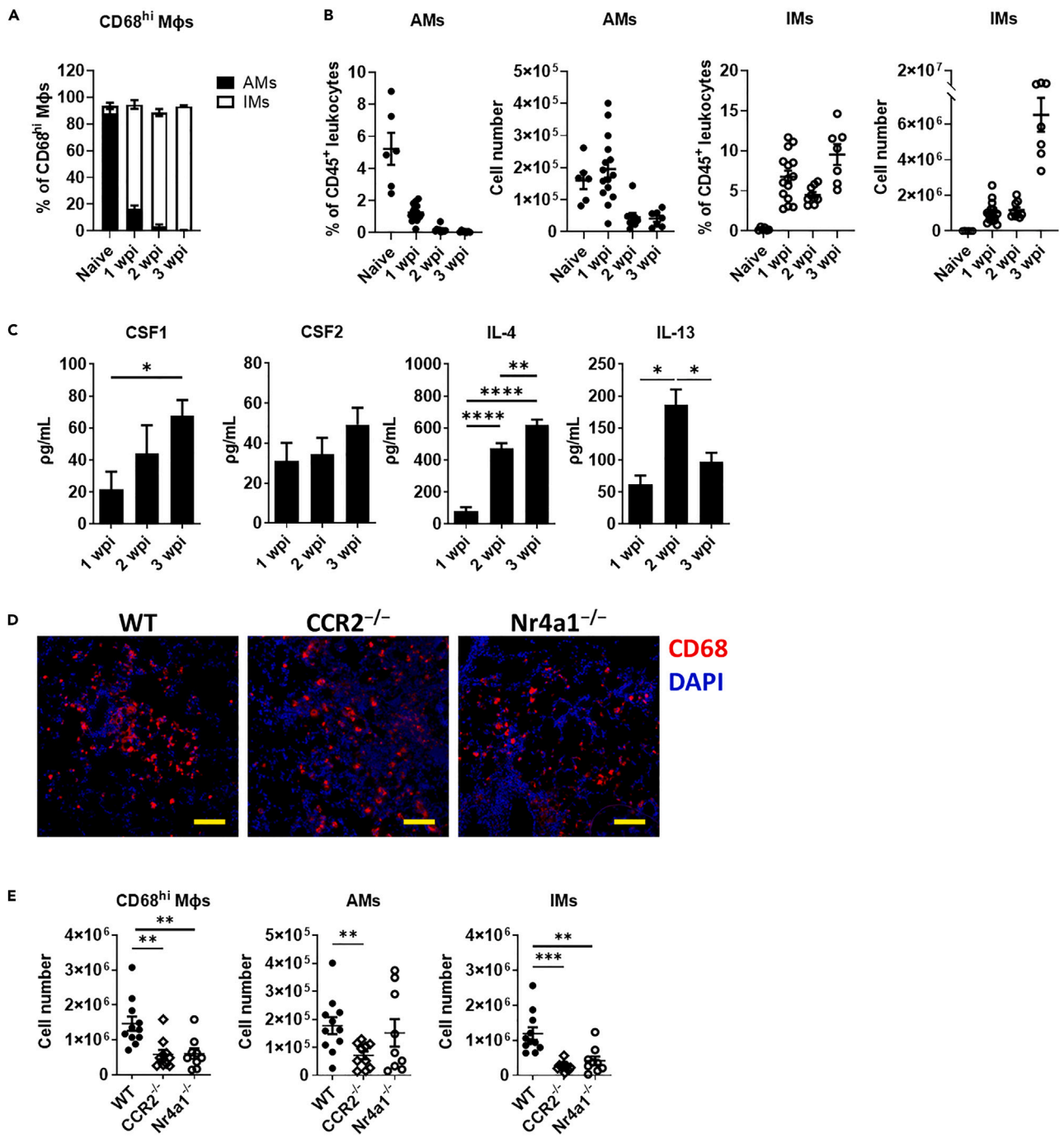


**Figure 3. Expansion of lung IMs correlates with enhanced CSF1 and IL-4 secretion and is reduced by the deficiency of CCR2 or Nr4a1 during infection with *C. neoformans***

(A and B) Quantification of the proportions of CD68$^{hi}$ AMs and IMs (A), and the percentages and cell numbers of AMs and IMs (B) in the lungs of naive (n = 6) and infected (n = 7–15) C57BL/6 mice at 1, 2, and 3 weeks PI. Data are expressed as mean ± SEM and are pooled from two independent experiments.

(C) The concentrations of CSF1, CSF2, IL-4, and IL-13 in the lungs of infected C57BL/6 mice (n = 4–6) at weeks 1, 2, and 3 PI as measured by ELISA. Data are expressed as mean ± SEM and are representative of three independent experiments.

(D) Representative immunohistochemistry images of CD68$^{+}$ cells (red) in the lungs of infected wild-type (WT) C57BL/6 mice, CCR2$^{-/-}$C57BL/6 mice, and Nr4a1$^{-/-}$C57BL/6 mice at 1-week PI. Nuclei were stained with DAPI (blue). Scale bars: 100 μm.

(E) Quantification of the numbers of CD68$^{hi}$ macrophages, AMs, and IMs in the lungs of infected WT (n = 11), CCR2$^{-/-}$ (n = 10), and Nr4a1$^{-/-}$ (n = 9) mice at 1-week PI. Data are expressed as mean ± SEM and are pooled from two independent experiments. *p < 0.05, **p < 0.01, ***p < 0.001, ****p < 0.0001.

and the percentage of IMs among CD68$^{hi}$ macrophages further increased during the remaining period of infection (Figure 3B).

A number of growth factors including CSF1 and CSF2, as well as Th2 cytokines such as IL-4 and IL-13 are known to promote expansion of tissue-resident macrophages.[39] To determine whether these factors promote lung macrophage expansion during infection with *C. neoformans*, we measured the concentrations of these cytokines in the lungs of infected mice and found that levels of CSF1, IL-4, and IL-13 were significantly increased (Figure 3C). The level of CSF2 also tended to increase in the lung during infection. We next blocked the CSF1 receptor (CSF1R) and the CSF2 receptor (CSF2R) using mAbs and found that blocking CSF1R significantly reduced the numbers of IMs but not AMs in the lungs at 1-week PI (Figure S1), confirming the role of CSF1 in the promotion of IM expansion during cryptococcal infection.

To determine whether recruited monocytes contributed to the expansion of IMs, we examined the accumulation of CD68$^{hi}$ macrophages, as well as AMs and IMs in the lungs of infected CCR2$^{-/-}$ and Nr4a1$^{-/-}$ mice, which have deficits in Ly6C$^{hi}$ and Ly6C$^{lo}$ monocytes, respectively.[33,40] As expected, CCR2$^{-/-}$ and Nr4a1$^{-/-}$ mice exhibited significantly lower numbers of Ly6C$^{hi}$ monocytes and Ly6C$^{lo}$ monocytes in the lung, respectively, during *C. neoformans* infection (Figure S2). We performed immunohistochemistry and found that the lungs of infected wild-type (WT) mice appeared to have more CD68$^{+}$ cells compared to infected CCR2$^{-/-}$ and Nr4a1$^{-/-}$ mice (Figure 3D). We then quantified the number of macrophages using flow cytometry. Interestingly, compared to infected WT mice, both infected CCR2$^{-/-}$ and Nr4a1$^{-/-}$ mice had significantly lower numbers of IMs (Figure 3E). These results suggest that deficiency of CCR2 or Nr4a1 affects the expansion of lung IMs.

## Lung AMs and IMs harbor *C. neoformans* during pulmonary infection

To better understand lung AM and IM responses to *C. neoformans*, we next examined how these cells interact with the fungal cells. In the lungs of mice infected with a GFP-expressing strain of *C. neoformans*, GFP$^{+}$ fungi were found to associate with CD68$^{hi}$ macrophages in a time-dependent manner (Figure 4A). At 1-week PI, approximately 60% of the leukocytes associated with *C. neoformans* were CD68$^{hi}$ macrophages, while the remaining 40% associated were non-macrophage cells, including CD68$^{lo}$ monocytes (Figure 4B). SiglecF$^{+}$ AMs isolated from the lungs of infected mice via bronchoalveolar lavage (BAL) were observed to have internalized *C. neoformans* in as little as 15 min (Figures 4C–4E). The percentage of AMs containing *C. neoformans* increased over time, with nearly 30% of isolated AMs having internalized at least one fungal cell by 24 h PI (Figure 4D). The number of internalized cryptococci also increased over time, with the average number of intracellular organisms ranging between 2 and 3 by 24 h (Figure 4E). Likewise, CD68$^{+}$CX3CR1$^{+}$ IMs were also observed to contain cryptococci cells at 1-week PI in whole lung sections (Figure 4F). These suggest that *C. neoformans* primarily interacts with macrophages in the lung, and that both AMs and IMs are able to internalize *C. neoformans*.

## Lung AMs and IMs are alternatively activated following infection with *C. neoformans*

The outcome of macrophage-*Cryptococcus* interactions is determined by the activation state of the host cells. Published studies have shown that fungal clearance is the result of M1 activation, while fungal persistence is associated with M2 polarization.[41–44] To gain insight into the polarization of lung AMs and IMs during cryptococcal infection, we next examined the expression of iNOS and Arg1 in AMs and IMs. A significantly higher proportion of AMs and IMs were Arg1$^{+}$ following infection, while the percentage of iNOS$^{+}$ macrophages decreased (Figure 5A). AMs and IMs both upregulated their expression of Arg1 and downregulated their expression of iNOS (Figure 5B). This resulted in significantly lower iNOS/Arg1 ratios in both AMs and IMs indicating an overall polarization toward M2 (Figure 5C). While both macrophages expressed similar levels of iNOS at all time points assessed, IMs expressed significantly higher amounts of Arg1 (Figure 5D). IMs also accounted for nearly 61% of all Arg1$^{+}$ leukocytes, and approximately 45% of the iNOS$^{+}$ leukocytes in the lung at 1-week PI (Figure 5E). This suggests that both AMs and IMs become alternatively activated during cryptococcal infection, and that IMs are more strongly polarized than their AM counterparts.

Since the use of Arg1 alone as an identifier of alternative activation has been somewhat controversial,[45] we also examined the expression Ym1 on CD68$^{+}$ cells in whole lung sections. The co-expression of Arg1 and Ym1 on CD68$^{+}$ cells (Figure 5F), along with the high expression of CD206 (Figure 2C), led us to conclude

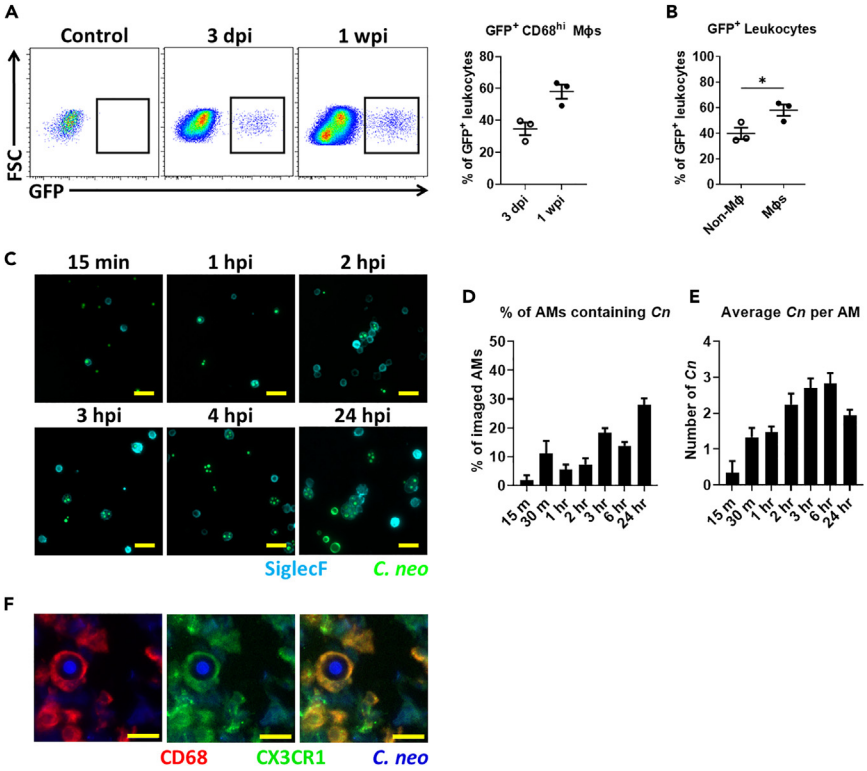


**Figure 4. AMs and IMs harbor *C. neoformans* in the lung**

(A) C57BL/6 mice were infected with a GFP-expressing strain of *C. neoformans*. Representative flow cytometry plots and quantification of $GFP^+$ $CD68^{hi}$ cells in the lungs of naive mice and infected mice at 3 days (n = 3) and 1 week (n = 3) PI. Data are expressed as mean ± SEM and are representative of two independent experiments.

(B) The quantification of the proportion of non-macrophage ($CD68^{lo/-}$) and macrophage ($CD68^{hi}$) associated with $GFP^+$ *C. neoformans* in infected mice at 1-week PI (n = 3). Data are expressed as mean ± SEM and are representative of two independent experiments.

(C) Representative immunofluorescence images of AMs (blue) isolated from C57BL/6 mice infected with a GFP-expressing strain of *C. neoformans* (green) at different time points via bronchoalveolar lavage (BAL). Scale bars: 100 μm.

(D) Quantification of the percentages of AMs containing at least one fungal cell at different time points. Data are expressed as mean ± SEM and are representative of one independent experiment.

(E) The quantification of the average number of *C. neoformans* per AM at different time points. Data are expressed as mean ± SEM and are representative of one independent experiment.

(F) Representative immunohistochemistry image of $CD68^+$ (red) $CX3CR1^+$ (green) cells harboring *C. neoformans* (blue) in the lungs of infected mice at 1-week PI. Scale bars: 20 μm; *p < 0.05.

that *C. neoformans* indeed induces M2 polarization of pulmonary AMs and IMs, with IMs being more highly polarized than AMs.

## Lung AMs promote fungal growth during infection with *C. neoformans*

We next performed functional studies to evaluate the contribution of lung AMs during *C. neoformans* infection. AMs, but not IMs, require CSF2 for development/survival.[15,46,47] Flow cytometry and immunohistochemistry demonstrated that $CSF2^{-/-}$ mice had significantly fewer AMs at steady state (Figure S3). Thus, we took advantage of the depletion of AMs in $CSF2^{-/-}$ mice and compared cryptococcal pathogenesis in $CSF2^{-/-}$ and WT mice during pulmonary infection. Compared to infected WT mice, infected $CSF2^{-/-}$ mice exhibited significantly lower AMs and fungal burdens in the lung, which correlated with a significant increase in survival time (Figures 6A–6C). Th2 cytokines have been previously shown to support resident macrophage development and functions.[39,48–51] Accordingly, we found that infected WT mice had significantly higher concentrations of Th2 cytokines including IL-4, IL-5, IL-10, and IL-13, but not Th1 cytokines including IFN-γ, IL-12, and TNF-α (Figure 6D). To further confirm the detrimental function of AMs during pulmonary *C. neoformans* infection, we specifically depleted AMs in WT mice through the intranasal

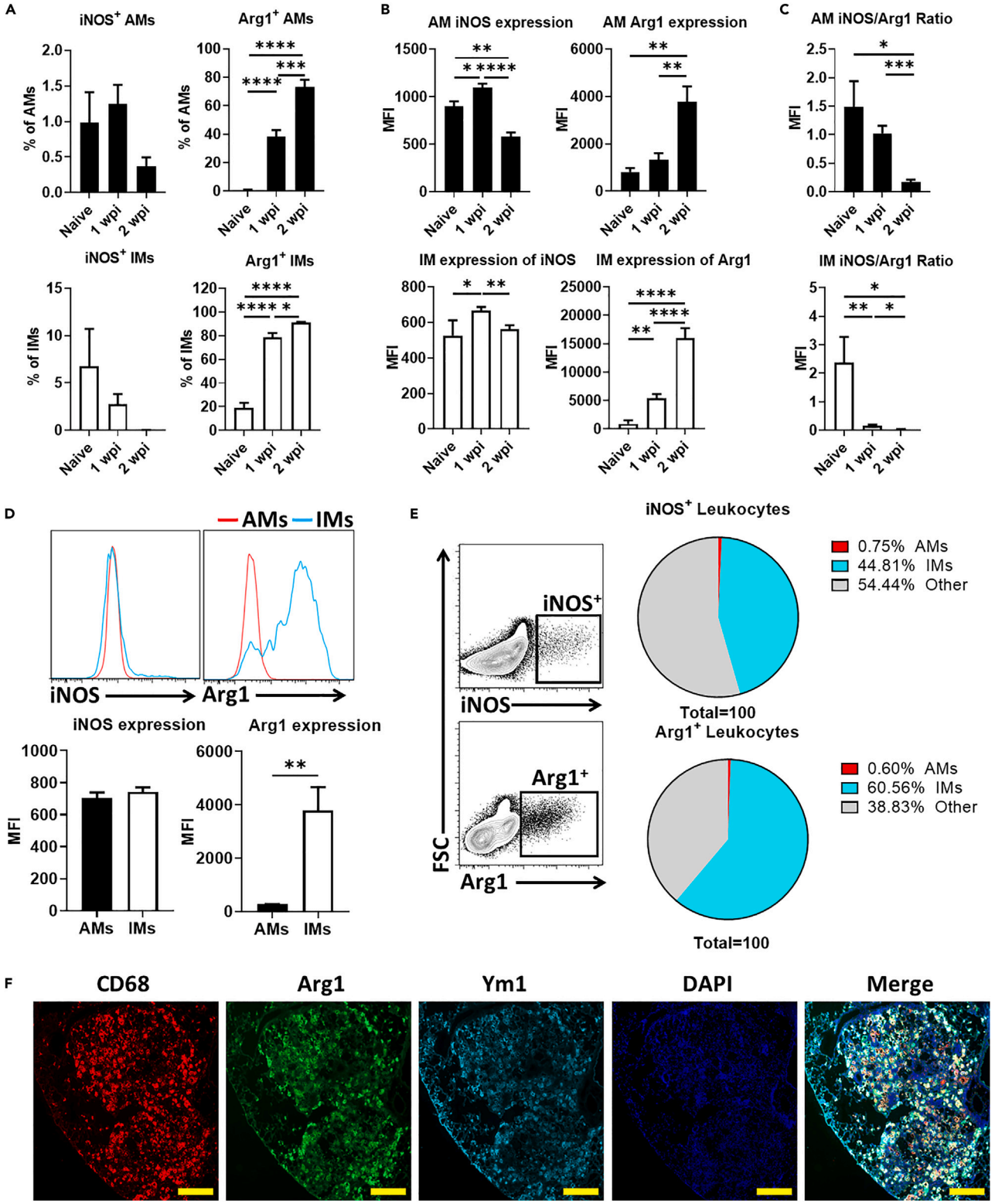


**Figure 5. AMs and IMs become alternatively activated in response to *C. neoformans***

(A) The percentage of iNOS$^+$ AMs and IMs and Arg1$^+$ AMs and IMs in naive mice (n = 5) and infected mice (n = 5–8) at weeks 1 and 2 PI. Data are expressed as mean ± SEM and are representative of two independent experiments.

**Figure 5. *Continued***

(B) The expression levels of iNOS and Arg1 in AMs and IMs expressed as median fluorescence intensity (MFI) in naive mice (n = 5) and infected mice (n = 5–8) at weeks 1 and 2 PI. Data are expressed as mean ± SEM and are representative of two independent experiments.

(C) The iNOS/Arg1 ratio in AMs and IMs in naive mice (n = 5) and infected mice (n = 5–8) at weeks 1 and 2 PI. Data are expressed as mean ± SEM and are representative of two independent experiments.

(D) Representative histograms and quantification of iNOS and Arg1 expression in AMs and IMs in infected mice (n = 4) at 1-week PI. Data are expressed as mean ± SEM and are representative of two independent experiments.

(E) Representative flow cytometry dot plots of $iNOS^+$ and $Arg1^+$ $CD45^+$ leukocytes and pie chart distribution of $iNOS^+$ and $Arg1^+$ leukocytes in the lungs of infected mice (n = 5–8) at 1-week PI. Data are expressed as mean ± SEM and are representative of two independent experiments.

(F) Representative immunohistochemistry images of $CD68^+$ (red), $Arg1^+$ (green), and $Ym1^+$ (teal) cells in the lungs of infected mice at 2 weeks PI. Nuclei were stained with DAPI (blue). Scale bars: 500 μm; *p < 0.05, **p < 0.01, ***p < 0.001, ****p < 0.0001.

administration of clodronate liposomes (CLL) prior to infection. CLL treatment reduced AM numbers by 67%, and depletion of AMs significantly reduced pulmonary fungal burdens during *C. neoformans* infection (Figure 6E). Collectively, these data indicate that AMs promote the growth and/or survival of *C. neoformans* in the infected lung.

### Lung IMs promote fungal growth during infection with *C. neoformans*

Finally, we sought to determine the function of IMs during pulmonary infection of *C. neoformans*. CSF1R has been recently shown to be highly expressed on all subsets of IMs compared to AMs.[14] Accordingly, unlike AMs, IMs require CSF1, but not CSF2, for development and survival.[15] Having demonstrated that anti-CSF1R mAbs reduced IM numbers (Figure S1), we next sought a strategy to deplete IMs by blocking CSF1-CSF1R signaling in mice. In this regard, PLX5622 has recently been used to deplete microglial cells through the inhibition of CSF1R.[52,53] Thus, we fed WT mice with a diet containing the CSF1R inhibitor PLX5622 for 7 days and found that this treatment was able to significantly reduce the number of IMs (elimination of 87% of IMs) in the lung at steady state (Figures 7A and 7B). This treatment did not affect the AM number in the lung and did not affect the expression of CD68 on AMs or IMs (Figure S4).

With this in mind, we fed mice PLX5622 diet for 7 days prior to infection with *C. neoformans* and continued to feed the mice PLX5622 diet during infection. We found that infected mice treated with PLX5622 diet displayed significantly lower fungal burdens in the lung at weeks 1, 2, and 3 PI, which was correlated with depletion of IMs in the infected lung (Figures 7C and 7D). In addition, the depletion of IMs by PLX5622 in infected mice was further confirmed using an alternative gating strategy and showed that IMs in the infected lung were significantly reduced, without affecting other subpopulations of lung leukocytes including AMs, DCs, neutrophils, eosinophils, $Ly6C^{hi}$ monocytes, $Ly6C^{lo}$ monocytes, NK cells, NKT cells, $CD4^+$ T cells, and $CD8^+$ T cells (Figure S5). Finally, the decrease in fungal burdens in the lung of PLX5622-treated mice was not due to off-target fungicidal effects of PLX5622, as the compound did not alter the growth or viability of *C. neoformans in vitro* (Figure S6).

Taken together, our data suggest that PLX5622 can deplete lung IMs and that depletion of IMs significantly reduces fungal burdens in the lung during pulmonary infection with *C. neoformans*.

## DISCUSSION

Lung macrophages consist mainly of AMs and IMs. Compared to AMs, less is known about IMs. Recent literature has identified multiple IM subsets based on their expression of various markers. Gibbings et al. divided IMs into three distinct populations referred to as IM1, IM2, and IM3.[14] IM1s were described as $CD11c^{lo}MHCII^{lo}$, while IM2s were $CD11c^{lo}MHCII^{hi}$ and IM3s were $CD11c^{hi}MHCII^{hi}$. Upon closer examination, it was revealed that IM1s and IM2s were likely the same cell type exhibiting different activation states, and have since been grouped together as IM1/IM2s.[54] Chakarov et al. identified two types of IMs by their expression of Lyve1 and MHC class II, referred to as $Lyve1^{hi}MHCII^{lo}$ and $Lyve1^{lo}MHCII^{hi}$ IMs.[16,17] Schyns et al. distinguished $CD206^+$ and $CD206^-$ IMs[16,17] and Ural et al. characterized $CD169^+$ nerve- and airway-associated IMs, also known as NAMs, and $CD169^-$ IMs.[15] These subpopulations arguably overlap with one another with IM1/IM2s corresponding to $Lyve1^{hi}MHCII^{lo}$, $CD206^+$ and $CD169^+$ IMs, and IM3s to $Lyve1^{lo}MHCII^{hi}$, $CD206^-$, and $CD169^-$ IMs. Transcriptional differences, as well as distinct anatomical niches, suggest that IM subsets differ in their behavior, though exactly how these cells function remains poorly understood. While IMs as a whole have been described as immunoregulatory through their production of the immunosuppressive cytokine IL-10,[18,19,55] IM1/IM2s in particular express higher levels of IL-10 as

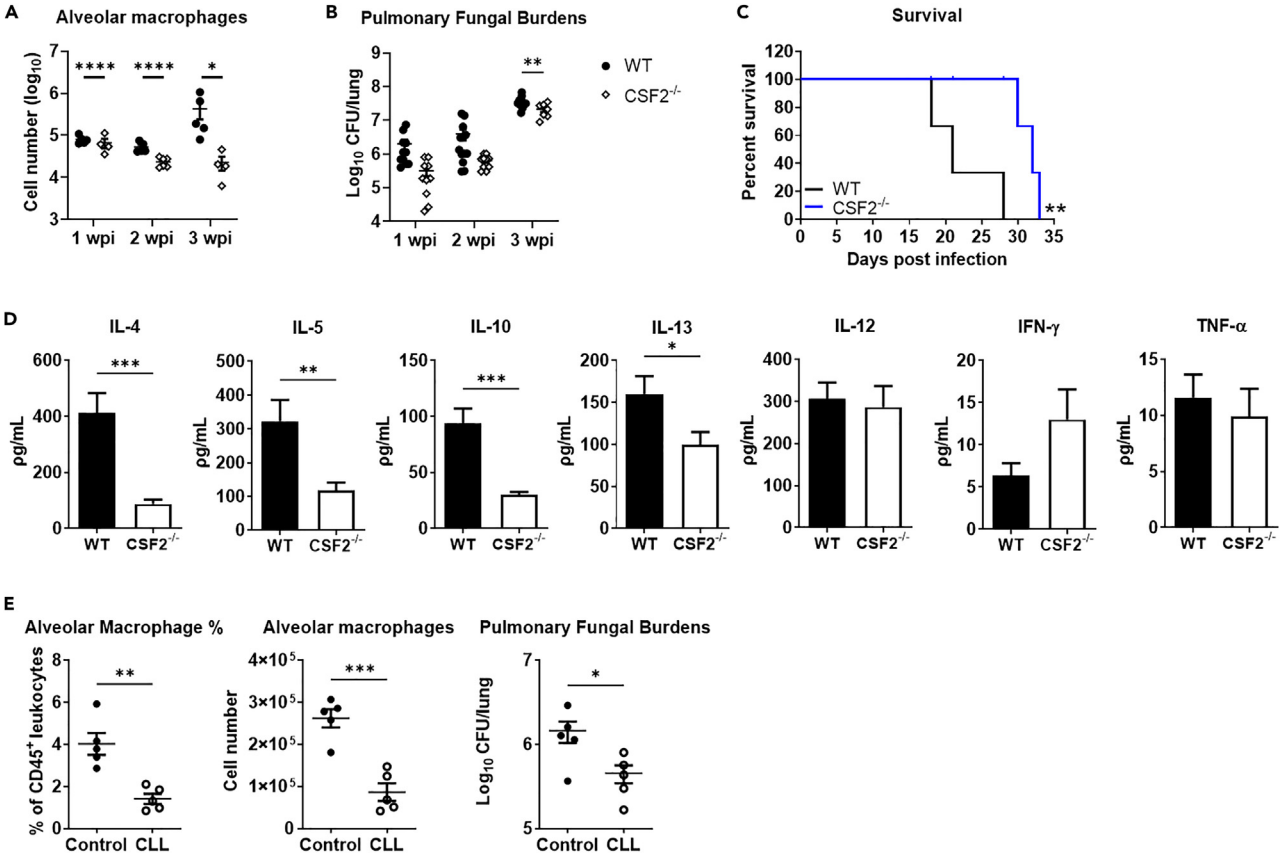


**Figure 6. AMs promote fungal growth in the infected lungs**

(A) WT and CSF2$^{-/-}$ C57BL/6 mice were infected intranasally with *C. neoformans*. Flow cytometry was performed to quantify the numbers of AMs in the lungs of infected WT (n = 5) and CSF2$^{-/-}$ (n = 4–6) mice at weeks 1, 2, and 3 PI. Data are expressed as mean ± SEM and are representative of three independent experiments.

(B) Fungal burdens in the lungs of infected WT (n = 10–13) and CSF2$^{-/-}$ (n = 7–10) mice at weeks 1, 2, and 3 PI. Data are expressed as mean ± SEM and are pooled from three independent experiments.

(C) Survival curve of infected WT (n = 6) (black line) and CSF2$^{-/-}$ (n = 6) (blue line) mice. Data are representative of two independent experiments.

(D) Th1 and Th2 cytokine concentrations in the lungs of infected WT (n = 5) and CSF2$^{-/-}$ (n = 5) mice at 2 weeks PI. Data are representative of one independent experiment.

(E) WT mice were treated intranasally with control or clodronate liposomes (CLL) and infected with *C. neoformans*. Quantification of the percentages and numbers of AMs in the lungs of control-treated (n = 5) and CLL-treated (n = 5) mice at 1-week PI, as well as the pulmonary fungal burdens at 1-week PI. Data are expressed as mean ± SEM and are representative of three independent experiments. *p < 0.05, **p < 0.01, ***p < 0.001, ****p < 0.0001.

well as other genes associated with repair.[16,17,37] IM3s, on the other hand, have increased expression of genes involved in antigen processing and presentation and defense response.[14,16,17,37]

As discussed above, previous characterizations of IMs have been focused on naive mice rather than infected mice. In this study, we instead studied IMs during infection and demonstrate that infection with *C. neoformans* induces the accumulation of CD68$^{hi}$ macrophages in the lungs of infected mice. These cells primarily consisted of two populations: a SiglecF$^{+}$CD11b$^{-}$ population and a SiglecF$^{-}$CD11b$^{+}$Ly6C$^{int}$CX3CR1$^{+}$ population. The former, identified as AMs, were distinguished by their high expression of CD68, SiglecF, CD11c, MerTK, and CD64 and their lack of CD11b. The latter were identified as IMs, based on their high expression of CX3CR1 along with other macrophage markers including MerTK, CD64, and F4/80.[19,56] Furthermore, *Cryptococcus*-induced IMs expressed high levels of CD11c and MHCII, suggesting these cells closely resembled IM3s. Their low expression of Lyve1 and CD169 further supported this. The fact that these cells were also CD206$^{+}$ though is in conflict with previously published literature that identified IM3s as CD206$^{-}$.[14] While CD206 is a cell surface marker on select macrophages at steady state,[16,57–60] it is also considered an indicator of M2 activation.[38] As such, it is possible that these IMs upregulate their expression of CD206 during cryptococcal infection

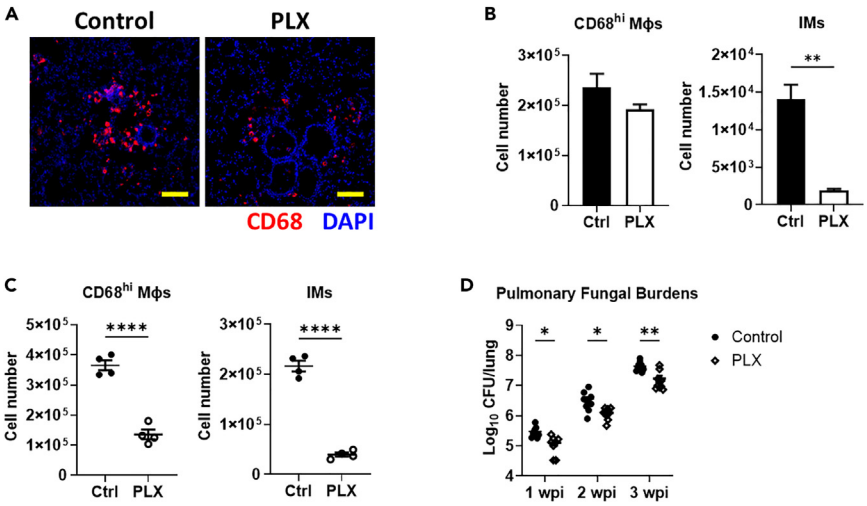


**Figure 7. IMs promote fungal growth in the infected lungs**

(A and B) C57BL/6 mice were fed control diet (Ctrl) or PLX5622-containing diet (PLX) for 7 days. Immunohistochemistry was performed to show $CD68^+$ cells (red) in the lungs of mice at steady state (A). Nuclei were stained with DAPI (blue). Scale bars: 100 μm. Flow cytometry was performed to quantify the numbers of $CD68^{hi}$ macrophages and IMs in the lungs of mice fed control diet (n = 3) or PLX5622-containing diet (n = 3) at steady state (B). Data are expressed as mean ± SEM and are representative of one independent experiment.

(C and D) C57BL/6 mice were fed control diet (Ctrl) or PLX5622-containing diet (PLX) for 7 days prior to intranasal infection with *C. neoformans* and were continually fed these diets during infection. Flow cytometry was performed to quantify the numbers of $CD68^{hi}$ macrophages and IMs in the lungs of infected mice fed control diet (n = 4) or PLX5622-containing diet (n = 4) at 1-week PI (C). Data are expressed as mean ± SEM and are representative of one independent experiment. The pulmonary fungal burdens were determined in infected mice fed control diet (n = 8–9) or PLX5622-containing diet (n = 9–10) at weeks 1, 2, and 3 PI (D). Data are expressed as mean ± SEM and are pooled from three independent experiments. *p < 0.05, **p < 0.01, ****p < 0.0001.

due to alternative activation. The characterization of IMs in a setting of infection in our study advanced our understanding of IMs in the context of infectious diseases.

Prior to infection, AMs represented a larger proportion of the $CD68^{hi}$ population, which is in line with reports that AMs are the most abundant macrophages in the lung at steady state.[60] Following infection though, IMs constituted more than 78% of all $CD68^{hi}$ cells in the lungs. This change in composition was the result of the rapid and dramatic increase in IM numbers. In a steady state, the replenishment of IMs depends on either *in situ* self-renewal[15] or differentiation of recruited monocytes.[16,17] In the setting of infection, Ural et al. reported that IMs proliferated robustly during influenza infection.[15] In addition, IMs were increased in a monocyte-dependent manner during *Mycobacterium tuberculosis* infection.[21] We found that *C. neoformans*-infected $CCR2^{-/-}$ and $Nr4a1^{-/-}$ mice exhibited significantly lower IMs. This suggests that recruited monocytes contributed, at least in part, to the expansion of IMs. In this context, a high level of monocyte chemoattractant protein 1 (MCP-1/CCL2) was detected during pulmonary *C. neoformans* infection.[30] Arguably, the IMs detected in mice infected with *C. neoformans* in our model included original tissue-resident IMs and IMs that recruited monocytes gave rise to in response to the infection. Interestingly, *C. neoformans*-induced expansion of IMs was correlated with enhanced secretion of CSF1 and Th2 cytokines including IL-4. Blocking CSF1R reduced IM numbers. CSF1 and IL-4 have been previously shown to directly signal resident macrophages to proliferate.[39,48–51] Thus, it is likely that the rapid expansion of IMs following *C. neoformans* infection is also partially attributed to local proliferation of IMs, in addition to the direct differentiation from recruited monocytes.

Following infection, both AMs and IMs were observed to ingest *C. neoformans*. As *C. neoformans* is a facultative intracellular pathogen,[61,62] internalization of the fungus can be either beneficial or detrimental to the host, depending on the status of macrophage activation.[63] Interestingly, both types of cells become alternatively activated, as evidenced by their upregulated expression of Arg1 and the increased percentage of $Arg1^+$ macrophages, along with expression of Ym1 and CD206, in response to *C. neoformans* infection. Of note, IMs were more strongly polarized to M2 compared to AMs during infection. Early studies have shown that, while alternatively activated macrophages can ingest cryptococci, they are likely inefficient killers.[63] In

this regard, a recent study demonstrated that a cryptococcal secreted protein (CPL1) promoted M2 polarization of IMs and that *C. neoformans* associated selectively with M2-polarized IMs.[36]

CSF2 is required for the development and survival of AMs, but not IMs.[15,46,47] Accordingly, very limited AMs were observed in CSF2$^{-/-}$ mice at steady state and during *C. neoformans* infection. Taking advantage of AM depletion by disrupting CSF2 signaling, we evaluated the effect of AMs on fungal growth and found that CSF2$^{-/-}$ mice infected with *C. neoformans* H99 exhibited significantly lower fungal burdens in the lung, associated with a longer survival. Clinical studies have shown that anti-CSF2 autoantibodies may put otherwise immunocompetent individuals at risk of developing meningitis caused by *Cryptococcus gattii* but not necessarily to that caused by *C. neoformans*.[64] CSF2 was secreted in significant concentrations in the cerebrospinal fluid of patients with HIV/AIDS co-infected with *C. neoformans*, though it was not associated with clinical outcome.[65] In animal models, early studies have shown that CSF2$^{-/-}$ mice displayed significantly higher fungal burdens in the lung, associated with impaired DC activation and reduced Th2/Th17 responses during infection with the less virulent strain *C. neoformans* 52D.[66,67] In contrast to the protective role of CSF2 during *C. neoformans* 52D infection, our results showing lower fungal burdens and prolonged survival in the absence of CSF2 signaling highlight a previously undescribed detrimental role of CSF2 during *C. neoformans* H99 infection. It is noteworthy that specific depletion of AMs by CLL also reduced lung fungal burdens, which demonstrated that AMs play a detrimental role during cryptococcal infection, probably by serving as an intracellular growth niche for the fungus. Thus, the detrimental effect of CSF2 is, at least in part, attributed to its function in supporting the development and survival of AMs, which likely facilitate the intracellular fungal growth in our model. Interestingly, we also found that infected WT mice had significantly higher secretions of Th2 cytokines including IL-4, as compared to infected CSF2$^{-/-}$ mice. Arguably, these Th2 cytokines, known to drive resident macrophage expansion,[39] played an important role in supporting the development/survival as well as M2 polarization of AMs during cryptococcal infection.

The CSF1R inhibitor PLX5622 has been used to deplete microglial cells in the brain for studying functions of these cells.[52,53] However, a recent study suggested that PLX5622 treatment may have off-target effects in other organs.[68] We found that mice treated with PLX5622 displayed significantly lower numbers of IMs without depletion of other subsets of leukocytes in the infected lung. Interestingly, infected mice depleted of IMs by PLX5622 exhibited significantly lower fungal burdens in the lungs, demonstrating a contribution of IMs to fungal growth during pulmonary infection with *C. neoformans*. It is likely that IMs promote fungal growth by providing an intracellular growth niche for *C. neoformans*. In support of our results, it has been previously reported that depletion of inflammatory monocytes enhanced the survival of *C. neoformans* H99-infected C57BL/6 mice, associated with reduced pulmonary fungal burdens.[35]

*C. neoformans* causes meningitis mainly in immunocompromised individuals including patients with HIV/AIDS, but also, rarely, in immunocompetent individuals.[1,69] Following infection, the immune system of healthy individuals can eliminate or contain the fungal cells in the lung, which is likely attributed to Th1/M1 responses.[31,70] In contrast, in patients with HIV/AIDS, *C. neoformans* grows in the lung, leading to brain dissemination and infection. Postmortem examination of human brain tissues showed that microglia are extremely distended due to numerous intracellular cryptococcal yeast cells,[71] suggesting intracellular growth of the fungus within macrophages. In clinical settings, brain fungal burden and patient death are linked to high cryptococcal phagocytosis by macrophages in HIV-associated cryptococcosis.[72] The current mouse model showing the detrimental functions of AMs and IMs shares some similarities with the clinical observations in patients with HIV/AIDS and thus may reflect, to some extent, the immune status of patients with HIV/AIDS infected with *C. neoformans*, but not immunocompetent individuals infected with *C. neoformans*.

## Limitations of the study

Although our study characterizing IM populations by flow cytometry was built on previously published findings which have identified and confirmed IM markers using scRNA-Seq, an independent scRNA-seq analysis of IMs in our model of *C. neoformans* infection would provide more informative insights into the expansion of IMs during cryptococcosis. In addition, our model showing detrimental effects of AMs and IMs may mimic some features occurring in patients with HIV/AIDS co-infected with *C. neoformans*, however, may not reflect Th1-dominated immune responses in immunocompetent individuals infected with *C. neoformans*. Furthermore, although we provided evidence that AMs and IMs harbored *C. neoformans*, we have not provided direct evidence that *C. neoformans* were growing within these macrophages *in vivo*. A future study using intravital microscopy may address this question.

## STAR★METHODS

Detailed methods are provided in the online version of this paper and include the following:

- KEY RESOURCES TABLE
- RESOURCE AVAILABILITY
  - Lead contact
  - Materials availability
  - Data and code availability
- EXPERIMENTAL MODEL AND SUBJECT DETAILS
  - Animals
- METHOD DETAILS
  - Fungal strains and culture
  - Infection models and treatments
  - Immunofluorescence staining
  - Flow cytometry
  - ELISA
  - Quantification of fungal burdens
- QUANTIFICATION AND STATISTICAL ANALYSIS

## SUPPLEMENTAL INFORMATION

Supplemental information can be found online at https://doi.org/10.1016/j.isci.2023.106717.

## ACKNOWLEDGMENTS

We thank Plexxikon Inc. for providing PLX5622. We thank Dr. Robin May (University of Birmingham) for providing *C. neoformans* H99 expressing GFP. National Institutes of Health (NIH) provided funding to M.S. under grant number AI131219 and AI131905. M.S. was also supported by the University of Maryland and Maryland Agricultural Experiment Station grants. A.B.S. was supported by NIH T32 training grant (AI089621). Y.C. was supported by the Basil & Anne Hatziolos Scholarship Fund for Veterinary Medical Research. The graphical abstract was created with BioRender.com.

## AUTHOR CONTRIBUTIONS

A.S. designed the study, performed experiments, performed data analyses, and wrote the manuscript; Y.C. performed experiments and analyzed the data. D.S. performed some initial experiments and contributed to the concept of the study. M.S. supervised the study and wrote the manuscript.

## DECLARATION OF INTERESTS

The authors declare no competing interests.

## INCLUSION AND DIVERSITY

We support inclusive, diverse, and equitable conduct of research.

Received: December 19, 2022
Revised: March 3, 2023
Accepted: April 18, 2023
Published: April 23, 2023

## REFERENCES

1. May, R.C., Stone, N.R.H., Wiesner, D.L., Bicanic, T., and Nielsen, K. (2016). *Cryptococcus*: from environmental saprophyte to global pathogen. Nat. Rev. Microbiol. *14*, 106–117. https://doi.org/10.1038/nrmicro.2015.6.

2. Velagapudi, R., Hsueh, Y.P., Geunes-Boyer, S., Wright, J.R., and Heitman, J. (2009). Spores as infectious propagules of *Cryptococcus neoformans*. Infect. Immun. *77*, 4345–4355. https://doi.org/10.1128/IAI.00542-09.

3. Strickland, A.B., and Shi, M. (2021). Mechanisms of fungal dissemination. Cell. Mol. Life Sci. *78*, 3219–3238. https://doi.org/10.1007/s00018-020-03736-z.

4. Denham, S.T., and Brown, J.C.S. (2018). Mechanisms of pulmonary escape and dissemination by *Cryptococcus neoformans*. J. Fungi *4*, 25. https://doi.org/10.3390/jof4010025.

5. Chen, Y., Shi, Z.W., Strickland, A.B., and Shi, M. (2022). *Cryptococcus neoformans* infection in the central nervous system: the battle between host and pathogen. J. Fungi *8*, 1069. https://doi.org/10.3390/jof8101069.

6. Casadevall, A. (2010). Cryptococci at the brain gate: break and enter or use a Trojan horse? J. Clin. Invest. *120*, 1389–1392. https://doi.org/10.1172/JCI42949.

7. McQuiston, T.J., and Williamson, P.R. (2012). Paradoxical roles of alveolar macrophages in the host response to *Cryptococcus neoformans*. J. Infect. Chemother. *18*, 1–9. https://doi.org/10.1007/s10156-011-0306-2.

8. Rajasingham, R., Smith, R.M., Park, B.J., Jarvis, J.N., Govender, N.P., Chiller, T.M., Denning, D.W., Loyse, A., and Boulware, D.R. (2017). Global burden of disease of HIV-associated cryptococcal meningitis: an updated analysis. Lancet Infect. Dis. *17*, 873–881. https://doi.org/10.1016/S1473-3099(17)30243-8.

9. Nelson, B.N., Hawkins, A.N., and Wozniak, K.L. (2020). Pulmonary macrophage and dendritic cell responses to *Cryptococcus neoformans*. Front. Cell. Infect. Microbiol. *10*, 10–37. https://doi.org/10.3389/fcimb.2020.00037.

10. Misharin, A.V., Morales-Nebreda, L., Mutlu, G.M., Budinger, G.R.S., and Perlman, H. (2013). Flow cytometric analysis of macrophages and dendritic cell subsets in the mouse lung. Am. J. Respir. Cell Mol. Biol. *49*, 503–510. https://doi.org/10.1165/rcmb.2013-0086MA.

11. Hu, G., and Christman, J.W. (2019). Editorial: alveolar macrophages in lung inflammation and resolution. Front. Immunol. *10*, 81–93. https://doi.org/10.1038/nri3600.

12. Liegeois, M., Legrand, C., Desmet, C.J., Marichal, T., and Bureau, F. (2018). The interstitial macrophage: a long-neglected piece in the puzzle of lung immunity. Cell. Immunol. *330*, 91–96. https://doi.org/10.1016/j.cellimm.2018.02.001.

13. Kopf, M., Schneider, C., and Nobs, S.P. (2015). The development and function of lung-resident macrophages and dendritic cells. Nat. Immunol. *16*, 36–44. https://doi.org/10.1038/ni.3052.

14. Gibbings, S.L., Thomas, S.M., Atif, S.M., McCubbrey, A.L., Desch, A.N., Danhorn, T., Leach, S.M., Bratton, D.L., Henson, P.M., Janssen, W.J., and Jakubzick, C.V. (2017). Three unique interstitial macrophages in the murine lung at steady state. Am. J. Respir. Cell Mol. Biol. *57*, 66–76. https://doi.org/10.1165/rcmb.2016-0361OC.

15. Ural, B.B., Yeung, S.T., Damani-Yokota, P., Devlin, J.C., de Vries, M., Vera-Licona, P., Samji, T., Sawai, C.M., Jang, G., Perez, O.A., et al. (2020). Identification of a nerve-associated, lung-resident interstitial macrophage subset with distinct localization and immunoregulatory properties. Sci. Immunol. *5*, eaax8756. https://doi.org/10.1126/sciimmunol.aax8756.

16. Schyns, J., Bai, Q., Ruscitti, C., Radermecker, C., De Schepper, S., Chakarov, S., Farnir, F., Pirottin, D., Ginhoux, F., Boeckxstaens, G., et al. (2019). Non-classical tissue monocytes and two functionally distinct populations of interstitial macrophages populate the mouse lung. Nat. Commun. *10*, 3964. https://doi.org/10.1038/s41467-019-11843-0.

17. Chakarov, S., Lim, H.Y., Tan, L., Lim, S.Y., See, P., Lum, J., Zhang, X.M., Foo, S., Nakamizo, S., Duan, K., et al. (2019). Two distinct interstitial macrophage populations coexist across tissues in specific subtissular niches. Science *363*, eaau0964. https://doi.org/10.1126/science.aau0964.

18. Makineni, S., Iyer, R., Sarangam, P., Newell, D., Zhao, L., Illikkal, R., Moses, J., Dewals, B., Thielen, C., Gustin, P., et al. (2006). Lung interstitial macrophages alter dendritic cell functions to prevent airway allergy in mice. J. Clin. Invest, 289–300. https://doi.org/10.1007/11945918_31.

19. Schyns, J., Bureau, F., and Marichal, T. (2018). Lung interstitial macrophages: past, present, and future. J. Immunol. Res. *2018*, 5160794. https://doi.org/10.1155/2018/5160794.

20. Tan, S.Y.S., and Krasnow, M.A. (2016). Developmental origin of lung macrophage diversity. Devenir *143*, 1318–1327. https://doi.org/10.1242/dev.129122.

21. Huang, L., Nazarova, E.V., Tan, S., Liu, Y., and Russell, D.G. (2018). Growth of Mycobacterium tuberculosis in vivo segregates with host macrophage metabolism and ontogeny. J. Exp. Med. *215*, 1135–1152. https://doi.org/10.1084/jem.20172020.

22. Patel, V.I., Booth, J.L., Duggan, E.S., Cate, S., White, V.L., Hutchings, D., Kovats, S., Burian, D.M., Dozmorov, M., and Metcalf, J.P. (2017). Transcriptional classification and functional characterization of human airway macrophage and dendritic cell subsets. J. Immunol. *198*, 1183–1201. https://doi.org/10.4049/jimmunol.1600777.

23. Nessa, K., Gross, N.T., Jarstrand, C., Johansson, A., and Camner, P. (1997). In vivo interaction between alveolar macrophages and *Cryptococcus neoformans*. Mycopathologia *139*, 1–7. https://doi.org/10.1023/A:1006843202124.

24. Tacker, J.R., Farhi, F., and Bulmer, G.S. (1972). Intracellular fate of *Cryptococcus neoformans*. Infect. Immun. *6*, 162–167. https://doi.org/10.1128/iai.6.2.162-167.1972.

25. Bolaños, B., and Mitchell, T.G. (1989). Killing of *Cryptococcus neoformans* by rat alveolar macrophages. Med. Mycol. *27*, 203–217. https://doi.org/10.1080/02681218980000291.

26. Shao, X., Mednick, A., Alvarez, M., van Rooijen, N., Casadevall, A., and Goldman, D.L. (2005). An innate immune system cell is a major determinant of species-related susceptibility differences to fungal pneumonia. J. Immunol. *175*, 3244–3251. https://doi.org/10.4049/jimmunol.175.5.3244.

27. Walsh, N.M., Botts, M.R., McDermott, A.J., Ortiz, S.C., Wüthrich, M., Klein, B., and Hull, C.M. (2019). Infectious particle identity determines dissemination and disease outcome for the inhaled human fungal pathogen *Cryptococcus*. PLoS Pathog. *15*, e1007777. https://doi.org/10.1371/journal.ppat.1007777.

28. Kechichian, T.B., Shea, J., and Del Poeta, M. (2007). Depletion of alveolar macrophages decreases the dissemination of a glucosylceramide-deficient mutant of *Cryptococcus neoformans* in immunodeficient mice. Infect. Immun. *75*, 4792–4798. https://doi.org/10.1128/IAI.00587-07.

29. Traynor, T.R., Kuziel, W.A., Toews, G.B., and Huffnagle, G.B. (2000). CCR2 expression determines T1 versus T2 polarization during pulmonary *Cryptococcus neoformans* infection. J. Immunol. *164*, 2021–2027. https://doi.org/10.4049/jimmunol.164.4.2021.

30. Osterholzer, J.J., Curtis, J.L., Polak, T., Ames, T., Chen, G.-H., McDonald, R., Huffnagle, G.B., and Toews, G.B. (2008). CCR2 mediates conventional dendritic cell recruitment and the formation of bronchovascular mononuclear cell infiltrates in the lungs of mice infected with *Cryptococcus neoformans*. J. Immunol. *181*, 610–620. https://doi.org/10.4049/jimmunol.181.1.610.

31. Leopold Wager, C.M., Hole, C.R., Wozniak, K.L., and Wormley, F.L. (2016). *Cryptococcus* and phagocytes: complex interactions that influence disease outcome. Front. Microbiol. *7*, 105–116. https://doi.org/10.3389/fmicb.2016.00105.

32. Osterholzer, J.J., Chen, G.-H., Olszewski, M.A., Curtis, J.L., Huffnagle, G.B., and Toews, G.B. (2009). Accumulation of CD11b + lung dendritic cells in response to fungal infection results from the CCR2-mediated recruitment and differentiation of ly-6C high monocytes. J. Immunol. *183*, 8044–8053. https://doi.org/10.4049/jimmunol.0902823.

33. Osterholzer, J.J., Chen, G.H., Olszewski, M.A., Zhang, Y.M., Curtis, J.L., Huffnagle, G.B., and Toews, G.B. (2011). Chemokine receptor 2-mediated accumulation of fungicidal exudate macrophages in mice that clear cryptococcal lung infection. Am. J. Pathol. *178*, 198–211. https://doi.org/10.1016/j.ajpath.2010.11.006.

34. Wiesner, D.L., Specht, C.A., Lee, C.K., Smith, K.D., Mukaremera, L., Lee, S.T., Lee, C.G., Elias, J.A., Nielsen, J.N., Boulware, D.R., et al. (2015). Chitin recognition via chitotriosidase promotes pathologic type-2 helper T cell responses to cryptococcal infection. PLoS Pathog. *11*, e1004701. https://doi.org/10.1371/journal.ppat.1004701.

35. Heung, L.J., and Hohl, T.M. (2019). Inflammatory monocytes are detrimental to the host immune response during acute infection with *Cryptococcus neoformans*. PLoS Pathog. *15*, e1007627. https://doi.org/10.1371/journal.ppat.1007627.

36. Dang, E.V., Lei, S., Radkov, A., Volk, R.F., Zaro, B.W., and Madhani, H.D. (2022). Secreted fungal virulence effector triggers allergic inflammation via TLR4. Nature *608*, 161–167. https://doi.org/10.1038/s41586-022-05005-4.

37. Shi, T., Denney, L., An, H., Ho, L.P., and Zheng, Y. (2021). Alveolar and lung interstitial macrophages: definitions, functions, and roles in lung fibrosis. J. Leukoc. Biol. *110*, 107–114. https://doi.org/10.1002/JLB.3RU0720-418R.

38. Mosser, D.M. (2003). The many faces of macrophage activation. J. Leukoc. Biol. *73*, 209–212. https://doi.org/10.1189/jlb.0602325.

39. Jenkins, S.J., and Allen, J.E. (2021). The expanding world of tissue-resident macrophages. Eur. J. Immunol. *51*, 1882–1896. https://doi.org/10.1002/eji.202048881.

40. Hanna, R.N., Carlin, L.M., Hubbeling, H.G., Nackiewicz, D., Green, A.M., Punt, J.A., Geissmann, F., and Hedrick, C.C. (2011). The transcription factor NR4A1 (Nur77) controls bone marrow differentiation and the survival of Ly6C- monocytes. Nat. Immunol. *12*, 778–785. https://doi.org/10.1038/ni.2063.

41. Hardison, S.E., Herrera, G., Young, M.L., Hole, C.R., Wozniak, K.L., and Wormley, F.L. (2012). Protective immunity against pulmonary cryptococcosis is associated with STAT1-mediated classical macrophage activation. J. Immunol. *189*, 4060–4068. https://doi.org/10.4049/jimmunol.1103455.

42. Hardison, S.E., Ravi, S., Wozniak, K.L., Young, M.L., Olszewski, M.A., and Wormley, F.L. (2010). Pulmonary infection with an interferon-γ-producing *Cryptococcus neoformans* strain results in classical macrophage activation and protection. Am. J. Pathol. *176*, 774–785. https://doi.org/10.2353/ajpath.2010.090634.

43. Stenzel, W., Müller, U., Köhler, G., Heppner, F.L., Blessing, M., McKenzie, A.N.J., Brombacher, F., and Alber, G. (2009). IL-4/IL-13-dependent alternative activation of macrophages but not microglial cells is associated with uncontrolled cerebral cryptococcosis. Am. J. Pathol. *174*, 486–496. https://doi.org/10.2353/ajpath.2009.080598.

44. Müller, U., Stenzel, W., Köhler, G., Werner, C., Polte, T., Hansen, G., Schütze, N., Straubinger, R.K., Blessing, M., McKenzie, A.N.J., et al. (2007). IL-13 induces disease-promoting type 2 cytokines, alternatively activated macrophages and allergic inflammation during pulmonary infection of mice with *Cryptococcus neoformans*. J. Immunol. *179*, 5367–5377. https://doi.org/10.4049/jimmunol.179.8.5367.

45. Briken, V., and Mosser, D.M. (2011). Editorial: switching on arginase in M2 macrophages. J. Leukoc. Biol. *90*, 839–841. https://doi.org/10.1189/jlb.0411203.

46. Guilliams, M., De Kleer, I., Henri, S., Post, S., Vanhoutte, L., De Prijck, S., Deswarte, K., Malissen, B., Hammad, H., and Lambrecht, B.N. (2013). Alveolar macrophages develop from fetal monocytes that differentiate into long-lived cells in the first week of life via GM-CSF. J. Exp. Med. *210*, 1977–1992. https://doi.org/10.1084/jem.20131199.

47. Schneider, C., Nobs, S.P., Kurrer, M., Rehrauer, H., Thiele, C., and Kopf, M. (2014). Induction of the nuclear receptor PPAR-γ by the cytokine GM-CSF is critical for the differentiation of fetal monocytes into alveolar macrophages. Nat. Immunol. *15*, 1026–1037. https://doi.org/10.1038/ni.3005.

48. Jenkins, S.J., Ruckerl, D., Thomas, G.D., Hewitson, J.P., Duncan, S., Brombacher, F., Maizels, R.M., Hume, D.A., and Allen, J.E. (2013). IL-4 directly signals tissue-resident macrophages to proliferate beyond homeostatic levels controlled by CSF-1. J. Exp. Med. *210*, 2477–2491. https://doi.org/10.1084/jem.20121999.

49. Muñoz-Garcia, J., Cochonneau, D., Télétchéa, S., Moranton, E., Lanoe, D., Brion, R., Lézot, F., Heymann, M.F., and Heymann, D. (2021). The twin cytokines interleukin-34 and CSF-1: masterful conductors of macrophage homeostasis. Theranostics *11*, 1568–1593. https://doi.org/10.7150/thno.50683.

50. Davies, L.C., Jenkins, S.J., Allen, J.E., and Taylor, P.R. (2013). Tissue-resident macrophages. Nat. Immunol. *14*, 986–995. https://doi.org/10.1038/ni.2705.

51. Jenkins, S.J., Ruckerl, D., Cook, P.C., Jones, L.H., Finkelman, F.D., Van Rooijen, N., MacDonald, A.S., and Allen, J.E. (2011). Local macrophage proliferation, rather than recruitment from the blood, is a signature of TH2 inflammation. Science *332*, 1284–1288. https://doi.org/10.1126/science.1204351.

52. Dagher, N.N., Najafi, A.R., Kayala, K.M.N., Elmore, M.R.P., White, T.E., Medeiros, R., West, B.L., and Green, K.N. (2015). Colony-stimulating factor 1 receptor inhibition prevents microglial plaque association and improves cognition in 3xTg-AD mice. J. Neuroinflammation *12*, 139. https://doi.org/10.1186/s12974-015-0366-9.

53. Elmore, M.R.P., Najafi, A.R., Koike, M.A., Dagher, N.N., Spangenberg, E.E., Rice, R.A., Kitazawa, M., Matusow, B., Nguyen, H., West, B.L., and Green, K.N. (2014). Colony-stimulating factor 1 receptor signaling is necessary for microglia viability, unmasking a microglia progenitor cell in the adult brain. Neuron *82*, 380–397. https://doi.org/10.1016/j.neuron.2014.02.040.

54. Koch, C.M., Chiu, S.F., Misharin, A.V., and Ridge, K.M. (2017). Lung interstitial macrophages: establishing identity and uncovering heterogeneity. Am. J. Respir. Cell Mol. Biol. *57*, 7–9. https://doi.org/10.1165/rcmb.2017-0150ED.

55. Sabatel, C., Radermecker, C., Fievez, L., Paulissen, G., Chakarov, S., Fernandes, C., Olivier, S., Toussaint, M., Pirottin, D., Xiao, X., et al. (2017). Exposure to bacterial CpG DNA protects from airway allergic inflammation by expanding regulatory lung interstitial macrophages. Immunity *46*, 457–473. https://doi.org/10.1016/j.immuni.2017.02.016.

56. Lee, J., Boyce, S., Powers, J., Baer, C., Sassetti, C.M., and Behar, S.M. (2020). CD11cHi monocyte-derived macrophages are a major cellular compartment infected by *Mycobacterium tuberculosis*. PLoS Pathog. *16*, e1008621. https://doi.org/10.1371/journal.ppat.1008621.

57. Mitsi, E., Kamng'ona, R., Rylance, J., Solórzano, C., Jesus Reiné, J., Mwandumba, H.C., Ferreira, D.M., and Jambo, K.C. (2018). Human alveolar macrophages predominately express combined classical M1 and M2 surface markers in steady state. Respir. Res. *19*, 66. https://doi.org/10.1186/s12931-018-0777-0.

58. Azad, A.K., Rajaram, M.V.S., and Schlesinger, L.S. (2014). Exploitation of the macrophage mannose receptor (CD206) in infectious disease diagnostics and therapeutics. J. Cytol. Mol. Biol. *1*, 1000003. https://doi.org/10.13188/2325-4653.1000003.

59. Allavena, P., Chieppa, M., Monti, P., and Piemonti, L. (2004). From pattern recognition receptor to regulator of homeostasis: the double-faced macrophaqe mannose receptor. Crit. Rev. Immunol. *24*, 179–192. https://doi.org/10.1615/CritRevImmunol.v24.i3.20.

60. Joshi, N., Walter, J.M., and Misharin, A.V. (2018). Alveolar macrophages. Cell. Immunol. *330*, 86–90. https://doi.org/10.1016/j.cellimm.2018.01.005.

61. Feldmesser, M., Kress, Y., Novikoff, P., and Casadevall, A. (2000). *Cryptococcus neoformans* is a facultative intracellular pathogen in murine pulmonary infection. Infect. Immun. *68*, 4225–4237. https://doi.org/10.1128/IAI.68.7.4225-4237.2000.

62. Feldmesser, M., Tucker, S., and Casadevall, A. (2001). Intracellular parasitism of macrophages by *Cryptococcus neoformans*. Trends Microbiol. *9*, 273–278. https://doi.org/10.1016/S0966-842X(01)02035-2.

63. Leopold Wager, C.M., and Wormley, F.L. (2014). Classical versus alternative macrophage activation: the Ying and the Yang in host defense against pulmonary fungal infections. Mucosal Immunol. *7*, 1023–1035. https://doi.org/10.1038/mi.2014.65.

64. Saijo, T., Chen, J., Chen, S.C.A., Rosen, L.B., Yi, J., Sorrell, T.C., Bennett, J.E., Holland, S.M., Browne, S.K., and Kwon-Chung, K.J. (2014). Anti-granulocyte-macrophage colony-stimulating factor autoantibodies are a risk factor for central nervous system infection by *Cryptococcus gattii* in otherwise immunocompetent patients. mBio *5*, e00912–e00914. https://doi.org/10.1128/mBio.00912-14.

65. Siddiqui, A., Brouwer, A.E., Wuthiekanun, V., Jaffar, S., Shattock, R., Irving, D., Sheldon, J., Chierakul, W., Peacock, S., Day, N., et al. (2005). IFN-Γ at the site of infection determines rate of clearance of infection in cryptococcal meningitis. J. Immunol. *174*, 1746–1750. https://doi.org/10.4049/jimmunol.174.3.1746.

66. Chen, G.-H., Teitz-Tennenbaum, S., Neal, L.M., Murdock, B.J., Malachowski, A.N., Dils, A.J., Olszewski, M.A., and Osterholzer, J.J. (2016). Local GM-CSF–dependent

differentiation and activation of pulmonary dendritic cells and macrophages protect against progressive cryptococcal lung infection in mice. J. Immunol. *196*, 1810–1821. https://doi.org/10.4049/jimmunol.1501512.

67. Chen, G.H., Olszewski, M.A., McDonald, R.A., Wells, J.C., Paine, R., Huffnagle, G.B., and Toews, G.B. (2007). Role of granulocyte macrophage colony-stimulating factor in host defense against pulmonary *Cryptococcus neoformans* infection during murine allergic bronchopulmonary mycosis. Am. J. Pathol. *170*, 1028–1040. https://doi.org/10.2353/ajpath.2007.060595.

68. Lei, F., Cui, N., Zhou, C., Chodosh, J., Vavvas, D.G., and Paschalis, E.I. (2020). CSF1R inhibition by a small-molecule inhibitor is not microglia specific; Affecting hematopoiesis and the function of macrophages. Proc. Natl. Acad. Sci. USA *117*, 23336–23338. https://doi.org/10.1073/pnas.1922788117.

69. Shi, Z.W., Chen, Y., Ogoke, K.M., Strickland, A.B., and Shi, M. (2022). Cryptococcal immune reconstitution inflammatory syndrome: from clinical studies to animal experiments. Microorganisms *10*, 2419. https://doi.org/10.3390/microorganisms10122419.

70. Lionakis, M.S., and Levitz, S.M. (2018). Host control of fungal infections: lessons from basic studies and human cohorts. Annu. Rev. Immunol. *36*, 157–191. https://doi.org/10.1146/annurev-immunol-042617-053318.

71. Lee, S.C., Dickson, D.W., and Casadevall, A. (1996). Pathology of cryptococcal meningoencephalitis: analysis of 27 patients with pathogenetic implications. Hum. Pathol. *27*, 839–847. https://doi.org/10.1016/S0046-8177(96)90459-1.

72. Sabiiti, W., Robertson, E., Beale, M.A., Johnston, S.A., Brouwer, A.E., Loyse, A., Jarvis, J.N., Gilbert, A.S., Fisher, M.C., Harrison, T.S., et al. (2014). Efficient phagocytosis and laccase activity affect the outcome of HIV-associated cryptococcosis. J. Clin. Invest. *124*, 2000–2008. https://doi.org/10.1172/JCI72950.

73. Strickland, A.B., Sun, D., Sun, P., Chen, Y., Liu, G., and Shi, M. (2022). IL-27 signaling promotes Th1 responses and is required to inhibit fungal growth in the lung during repeated exposure to *Aspergillus fumigatus*. Immunohorizons *6*, 78–89. https://doi.org/10.4049/immunohorizons.2100117.

## STAR★METHODS

### KEY RESOURCES TABLE

| REAGENT or RESOURCE | SOURCE | IDENTIFIER |
|---|---|---|
| Antibodies | | |
| anti-CD45 | BioLegend | Clone 30-F11 |
| anti-CD206 | BioLegend | Clone C068C2 |
| anti-CD11c | BioLegend | Clone N418 |
| anti-MerTK | BioLegend | Clone 2B10C42 |
| anti-CD64 | BioLegend | Clone X54-5/7.1 |
| anti-SiglecF | BioLegend | Clone S17007L |
| anti-CD11b | BioLegend | Clone M1/70 |
| anti-Ly6C | BioLegend | Clone HK1.4 |
| anti-CX3CR1 | BioLegend | Clone SA011F11 |
| anti-F4/80 | BioLegend | Clone BM8 |
| anti-MHC class II | BioLegend | Clone M5/114.15.2 |
| anti-CD169 | BioLegend | Clone 3D6.112 |
| anti-Lyve1 | eBioscience | Clone ALY7 |
| anti-CD68 | BioLegend | Clone FA-11 |
| anti-iNOS | BioLegend | Clone W16030C |
| anti-Arg1 | ThermoFischer | Clone A1exF5 |
| anti-CSF1R | Bio X Cell | Clone AFS98 |
| anti-CSF2R | Bio X Cell | Clone MPI-22E9 |
| Biological samples | | |
| *Cryptococcus neoformans* serotype A strain H99 | ATCC | ATCC 208821 |
| GFP-expressing *Cryptococcus neoformans* serotype A strain H99 | Dr. Robin May (University of Birmingham, United Kingdom) | PMID: 21209844; https://doi.org/10.1371/journal.pone.0015968 |
| Chemicals, peptides, and recombinant proteins | | |
| PLX5622 | Plexxikon Inc | N/A |
| Clodronate liposome (Clodrosome®) | Encapsula Nanosciences | SKU# CLD-8901 |
| Control liposome (Encapsome®) | Encapsula Nanosciences | SKU# CLD-8901 |
| Critical commercial assays | | |
| Mouse M-CSF DuoSet ELISA | R&D Systems | Catalog # DY416-05 |
| Mouse GM-CSF DuoSet ELISA | R&D Systems | Catalog # DY415-05 |
| BD OptEIA Mouse IL-4 ELISA Set | BD Biosciences | Cat No: 555232 |
| IL-13 Mouse Uncoated ELISA Kit | Invitrogen | Catalog # 88-7137-88 |
| BD OptEIA Mouse IL-5 ELISA Set | BD Biosciences | Cat No: 555236 |
| BD OptEIA Mouse IL-10 ELISA Set | BD Biosciences | Cat No: 555252 |
| BD OptEIA Mouse IL-12 p40 ELISA Set | BD Biosciences | Cat No: 555165 |
| BD OptEIA Mouse IFN-γ ELISA Set | BD Biosciences | Cat No: 555138 |
| TNF alpha Mouse Uncoated ELISA Kit | Invitrogen | Catalog # 88-7324-88 |
| Experimental models: Organisms/strains | | |
| C57BL/6 mice | National Cancer Institute | 556NCIC57BL/ |
| CCR2$^{-/-}$ mice | The Jackson Laboratory | JAX: 004999 |

(*Continued on next page*)

*Continued*

| REAGENT or RESOURCE | SOURCE | IDENTIFIER |
|---|---|---|
| Nr4a1$^{-/-}$ mice | The Jackson Laboratory | JAX: 006187 |
| CSF2$^{-/-}$ mice | The Jackson Laboratory | JAX: 026812 |
| Software and algorithms | | |
| FlowJo v.7.6 | TreeStar | https://www.flowjo.com/ |
| Prism | GraphPad | https://www.graphpad.com/ |

## RESOURCE AVAILABILITY

### Lead contact

Further information and requests for resources and reagents should be directed to and will be fulfilled by the lead contact, Meiqing Shi (mshi@umd.edu).

### Materials availability

This study did not generate new unique reagents.

### Data and code availability

- All data reported in this paper will be shared by the lead contact upon reasonable request.
- No original code was reported in this study.
- Additional information required to reanalyze the data reported in this paper is available from the lead contact upon request.

## EXPERIMENTAL MODEL AND SUBJECT DETAILS

### Animals

C57BL/6 mice were purchased from the National Cancer Institute (Frederick, MD) for use as wild-type mice and were housed in the animal facilities at the University of Maryland, College Park prior to use in experiments. CCR2$^{-/-}$ mice (Strain #: 004999), Nr4a1$^{-/-}$ mice (Strain #: 006187), and CSF2$^{-/-}$ mice (Strain #: 026812), all in the C57BL/6 background were purchased from The Jackson Laboratory (Bar Harbor, ME, USA), and bred in-house. All mice were maintained in specific-pathogen-free conditions in individually ventilated cages with a standard 12 h light/dark cycle. For experiments, age- and sex-matched, male or female 6- to 8-week-old mice were used. The study protocol was approved by the Institutional Animal Care and Use Committee (IACUC) at the University of Maryland, College Park. All animal studies were conducted in accordance with the National Institutes of Health guidelines.

## METHOD DETAILS

### Fungal strains and culture

The highly virulent *Cryptococcus neoformans* serotype A strain H99 (208821) was purchased from ATCC (Manassas, Virginia) and used for all experiments. The GFP-expressing *C. neoformans* H99 strain (H99-GFP) was a gift from Dr. Robin May (University of Birmingham, United Kingdom). Fungi were cultured from frozen stocks on Sabouraud dextrose agar (Difco) plates for 2 days at 30°C, prior to inoculation into Sabouraud dextrose broth (Difco). Cultures were grown to log phase with shaking at 200 rpm at 30°C for 16 hours. Fungi were washed twice and resuspended in sterile PBS. To examine the effects of PLX5622 on fungal growth and survival, control diet pellets or PLX5622 diet pellets were dissolved in 15 mL of Sabouraud dextrose broth until saturation was achieved. Any remaining diet debris was allowed to sediment, and the saturated broth was decanted off into new 50 mL conical tubes. $7.5x10^7$ *C. neoformans* H99 fungal cells were inoculated into each tube from a liquid culture grown the night before, and cultures were grown with shaking at 200 rpm at 30°C for 16 hours. Fungal cells were counted directed using a hemacytometer, and 10 μL of culture were serially diluted using sterile water and 10 μL replicates were plated on Sabouraud dextrose agar. Plates were incubated overnight at 30°C and colony forming units (CFUs) were counted and the total fungal concentration in the presence or absence of PLX5622 was calculated.

### Infection models and treatments

Infections were performed by intranasal inoculation of $1x10^4$ fungal cells suspended in 30 μL of sterile PBS. Animals were anesthetized by intraperitoneal injection of a mixture containing ketamine (100 mg/kg) and xylazine (10 mg/kg). Mice were maintained in an upright position for 5 mins to allow for the complete inhalation of the fungal suspension into the lungs. To deplete AMs, mice were anesthetized and treated intranasally with 80 μL of control liposome or clodronate liposome (Encapsula Nanosciences) prior to infection with *C. neoformans*. For IM depletion, mice were fed a diet (Research Diets Inc.; New Brunswick, New Jersey) containing 1200 mg/kg of the CSF1R inhibitor PLX5622 (Plexxikon Inc.; San Francisco, California) for 7 days prior to infection and were continually fed these diets during infection. To block CSFRs, 100 μg of anti-CSF1R (AFS98), anti-CSF2R (MPI-22E9) (Bio X Cell) or PBS was injected into the peritoneal cavity of mice at the time of infection, and was readministered every 2 to 3 days until sample collection.

### Immunofluorescence staining

To stain whole lung sections, mice were overdosed using a mix of ketamine (100 mg/kg) and xylazine (10 mg/kg) and were perfused with 10 mL of 4% paraformaldehyde (PFA). Lungs were inflated with 1 mL of 50% optimal cutting temperature (OCT) compound (Fischer) in PBS and were removed and embedded and frozen in 100% OCT. Frozen tissues were cut into 7 μm thick slices. Prior to staining, slides were fixed in ice cold acetone at 4°C for 10 mins, and were blocked with 5% goat serum in PBS for 30 mins at room temperature in a humidity chamber. Afterward, samples were incubated with fluorophore-conjugated antibodies including anti-CD68, anti-CD206, anti-CD11c, anti-CX3CR1, anti-SiglecF, anti-Arg1 and anti-Ym1 at a 1:200 dilutions overnight at 4°C. Samples were then washed, and either nuclei were stained using DAPI or fungi were stained with Uvitex 2B. For weak markers, signal was amplified by incubating samples with fluorophore-conjugated secondary antibodies (1:1000) prior to staining with DAPI/Uvitex 2B.

To stain AMs, mice infected intranasally with $1x10^6$ H99-GFP, were anesthetized and bronchoalveolar lavage (BAL) was performed at various time points. BAL fluid was centrifuged, and the pellet washed and resuspended in 100 μL of flow cytometry staining buffer. AMs were stained with fluorophore-conjugated anti-SiglecF for 20 mins and washed and resuspended in 10 μL of buffer. All samples were visualized under a Zeiss Axio Examiner.Z1 fluorescence microscope at a magnification of 20x.

### Flow cytometry

To isolate lung leukocytes, lungs were collected into 1 mL of sterile RPMI 1640 medium in a 24-well plate and minced with surgical scissors, followed by digestion with collagenase IV (Worthington Biochemical) at a final concentration of 1 mg/mL for 45 min at 37°C with gentle shaking. Tissues were then manually homogenized on ice through a 70-μm cell strainer, followed by centrifugation at 500 × *g* for 5 min at 4°C. The cells were collected to 37% Percoll (GE Healthcare Biosciences) and subjected to gradient centrifugation at 1200 × *g* for 15 min at room temperature with the brake off. Red blood cells were lysed by ACK (ammonium-chloride-potassium) lysing buffer (5–10 min at room temperature). After one wash with sterile PBS, cells were resuspended in in flow cytometry staining buffer (1% BSA in PBS with 0.05% sodium azide) and then counted using a hemocytometer.[73]

$1x10^6$ lung leukocytes were resuspended in 100 μL of flow cytometry staining buffer (1% BSA in PBS with 0.05% sodium azide) and incubated with anti-CD16/32 mAb (93) for 20 mins at 4°C to block Fc receptors. Cell surface markers were then stained with fluorophore-conjugated antibodies including anti-CD45 (30-F11), anti-CD206 (C068C2), anti-CD11c (N418), anti-MerTK (2B10C42), anti-CD64 (X54-5/7.1), anti-SiglecF (S17007L), anti-CD11b (M1/70), anti-Ly6C (HK1.4), anti-CX3CR1 (SA011F11), anti-F4/80 (BM8), anti-MHC class II (M5/114.15.2), anti-CD169 (3D6.112), anti-Lyve1 (ALY7; eBioscience). Cells were washed, fixed and permeabilized using the Foxp3/Transcription Factor Staining Buffer Set (eBioscience) according to the manufacturer's protocols, and intracellular proteins stained with fluorophore-conjugated antibodies including anti-CD68 (FA-11), anti-iNOS (W16030C) and anti-Arg1 (A1exF5; ThermoFischer). Cells were then washed and resuspended in 300 μL of staining buffer. Samples were detected with a FACSCanto II flow cytometer (BD Biosciences) and data analyzed using FlowJo v.7.6 (TreeStar). All antibodies used for flow cytometry were purchased from BioLegend, unless otherwise stated.

### ELISA

Supernatants from lung homogenates (1 ml per lung) were collected during leukocyte isolation and stored at −80°C. Prior to use, samples were thawed and centrifuged to pellet any debris. The remaining suspensions were used to measure the concentrations of various cytokine including CSF1 (R&D Systems), CSF2 (R&D Systems), IL-4 (BD), IL-13 (eBioscience), IL-5 (BD), IL-10 (BD), IL-12p40 (BD), IFN-γ (BD) and TNF-α (ThermoFischer). All kits were used according to the manufacturer's protocols and ELISA plates were read using a BioTek Synergy HTX plate reader.

### Quantification of fungal burdens

10 μL portions of lung homogenates were collected and reserved following homogenization during leukocyte isolation. Samples were subjected to serial dilutions using sterile water and 10 μL replicates were plated on Sabouraud dextrose agar. Plates were incubated overnight at 30°C and colony forming units (CFUs) were counted and the total fungal burden per organ calculated.

## QUANTIFICATION AND STATISTICAL ANALYSIS

All data were expressed as mean ± SEM. Statistical tests were performed using GraphPad Prism (San Diego, CA). For data sets containing two groups, the unpaired Student's *t*-test was used to determine significance. For comparisons of more than two groups, own-way analysis of variance (ANOVA) was performed followed by Tukey's post-hoc test. For survival, log-rank tests were used for comparisons. A $p$ value of $p < 0.05$ was considered to be statistically significant.